DAMAGE IDENTIFICATION FROM THE VIBRATION CHARACTERISTICS IN PLATES BY FLEXIBILITY MATRIX

Rosilene Abreu Portella Corrêa, rosileneportella@id.uff.br
Universidade Federal Fluminense
Leonardo Tavares Stutz, ltstutz@iprj.uerj.br
Universidade do Estado do Rio de Janeiro
Roberto Aizik Tenenbaum, tenenbaum@iprj.uerj.br
Universidade do Estado do Rio de Janeiro

Abstract. *In this work a model for damage identification in plates from the vibration characteristics based on the structural flexibility matrix is presented. The method has been developed to identify and quantify damage in rectangular plates. It is assessed by considering changes in the reduced flexibility matrix of the structure, which is only related to the measured degrees of freedom and may be accurately estimated from a few of the lower frequency modes in a modal test. The main idea is that modal parameters are a function of the physical properties of the structure. The finite elements method (FEM) is used to model a rectangular plate and the damage field. The Luus-Jaakola optimization method is applied to minimize the difference between the flexibility matrix obtained from modal testing and the analytical flexibility matrix. The Luus-Jaakola optimization method presented good results, however with a high computational cost. The flexibility matrix itself was used to provide an estimation of the damage localization. The objective is to minimize the number of parameters updated for the Luus-Jaakola method and the computacional cost for the correct identification of the damage. Some numeric examples for different damages scenaries are presented.*

Keywords: *Damages identification in plates, Matrix flexibility, Luus-Jaakola method.*

1. INTRODUCTION

Several phenomena can cause damage to a structure and thus compromise its proper operation and endanger people's lives, like impacts, actions of wind, people and vehicle's moving etc.

For the security of people and structures, many authors have used dynamic tests to determine characteristics of the structure vibration, such as frequencies, modes and modal damping, in order to evaluate possible structural failure (Alvandi & Cremona, 2006, Jauregui & Farrar, 1996, Chang *et al.*, 2003, Carrilo & Laier, 2006). The basic thought for this methodology is that the modal parameters are functions of the physical properties of the structure (mass, stiffness and damping) and therefore changes in physical properties will be reflected in the modal properties, which in turn can be obtained in an experimental trial and used to deduce about the damage. The structural damage identification in its initial stage and the continuous monitoring of the structure contribute to the reduction of maintenance or repair costs, and increase its reliability and lifetime.

In this paper, the finite element method is used to model a rectangular plate, where the damage in the structure is described through a cohesion parameter (Stutz, 2005). The inverse problem of identifying structural damage is defined as a minimization problem, where a set of cohesion parameters is determined to minimize a functional based on the difference between the experimental flexibility matrix and the one provided by the finite element model. The Luus-Jaakola optimization method was used to solve the inverse problem of damage identification.

2. MATHEMATICAL MODEL

From an appropriate spatial discretization, using the finite element method, the equation of motion of the structure is given by

$$\mathbf{M}\ddot{\mathbf{u}} + \mathbf{C}\dot{\mathbf{u}} + \mathbf{K}\mathbf{u} = \mathbf{f}, \tag{1}$$

where **M**, **K** and **C** are, respectively, the matrices of mass, stiffness and damping, with dimension of $n \times n$, **u** is a $n \times 1$ vector of generalized displacements and **f** is a $n \times 1$ vector of generalized forces.

The undamped natural frequencies and mode shapes of the structure can be obtained from the eigenvalue-eigenvector problem,

$$(\mathbf{K} - \boldsymbol{\omega}_i^2\mathbf{M})\boldsymbol{\phi}_i = 0, \tag{2}$$

where $\boldsymbol{\omega}_i$ e $\boldsymbol{\phi}_i$ refers, respectively, to the *i-th* natural frequency and to the *i-th* mode shape of the structure.

Considering the mode shapes of the structure normalized with respect to the mass matrix, one has

$$\boldsymbol{\Phi}^{\mathrm{T}}\mathbf{M}\boldsymbol{\Phi} = \mathbf{I}; \tag{3}$$

$$\mathbf{\Phi}^{\mathrm{T}}\mathbf{K}\mathbf{\Phi} = \mathbf{\Lambda}, \tag{4}$$

where $\mathbf{\Phi}$ is the modal matrix and T means the transpose, $\mathbf{I}$ is the identity matrix and $\mathbf{\Lambda}$ is a diagonal matrix consisted of the squared values of the natural frequencies. According to Eq. 4, the stiffness matrix can be written as

$$\mathbf{K} = (\mathbf{\Phi}\mathbf{\Lambda}^{-1}\mathbf{\Phi}^{\mathrm{T}})^{-1}. \tag{5}$$

The flexibility matrix $\mathbf{G}$ of a structure is defined as the inverse of its stiffness matrix and, therefore, it can be written in terms of the modal parameters as

$$\mathbf{G} = (\mathbf{\Phi}\mathbf{\Lambda}^{-1}\mathbf{\Phi}^{\mathrm{T}}). \tag{6}$$

Considering Eq. (6), the flexibility matrix can be rewritten as

$$\mathbf{G} = \sum_{i=1}^{n} \frac{1}{{\boldsymbol{\omega}_i}^2}\boldsymbol{\phi}_i \otimes \boldsymbol{\phi}_i, \tag{7}$$

where $\otimes$ stands for the tensor product.

The Eq. (7) shows that the modal contribution to the flexibility matrix decreases with the increasing of the frequency, which characterizes a great advantage to the use of the flexibility matrix for damage identification purposes, since modes of higher frequencies are more difficult to obtain in a modal test. Due to pratical limitations, the following flexibility matrix can be obtained from an experimental test.

$$\bar{\mathbf{G}}_{\mathrm{exp}} = \sum_{i=1}^{n_{\mathrm{exp}}} \frac{1}{\boldsymbol{\omega}^2_{\mathrm{i,exp}}}\boldsymbol{\phi}_{\mathrm{i,exp}} \otimes \boldsymbol{\phi}_{\mathrm{i,exp}}, \tag{8}$$

where n_{exp} is the number of modes obtained from the modal test and $\phi_{i,\mathrm{exp}}$ and $\omega_{i,\mathrm{exp}}$ are, respectively, the *i-th* mode shape and *i-th* natural frequency, determined only in a subset of m degrees of freedom of the structure. From Eq. (8), it should be noted that the size of the matrix $\bar{\mathbf{G}}_{\mathrm{exp}}$ depends only on the number m of degrees of freedom (DOF) which were measured in the experiment.

To obtain an inverse relation between the analytical flexibility matrix $\bar{\mathbf{G}}$, related only to the m DOF measured in the vibration test, and a matrix of the same size, containing information about the stiffness properties of the structure, the original stiffness matrix must be partitioned

$$\mathbf{K} = \begin{bmatrix} \mathbf{K}_{\mathrm{mm}} & \mathbf{K}_{\mathrm{mo}} \\ \mathbf{K}^T_{\mathrm{mo}} & \mathbf{K}_{\mathrm{oo}} \end{bmatrix}, \tag{9}$$

where T means transposed, and the subscripts m and o refer, respectively, to the DOF measured and omitted. It can be seen (Alvin *et al.*, 1995) that a reduced flexibility matrix $\bar{\mathbf{G}}$, Eq. (10), may be obtained as the inverse of the reduced stiffness matrix, obtained by Static Guyan Reduction (Guyan, 1965),

$$\bar{\mathbf{G}} = \bar{\mathbf{K}}^{-1} = [\mathbf{K}_{\mathrm{mm}} - \mathbf{K}_{\mathrm{mo}}\mathbf{K}^{-1}_{\mathrm{oo}}\mathbf{K}^T_{\mathrm{mo}}]. \tag{10}$$

In this paper, the measure of cohesion β is used to describe the behavior of the damage in the structure. This parameter is related to the connection between the material points and can be interpreted as a measure of the state of local cohesion of the material, where $0 \leq \beta \leq 1$. If $\beta = 1$, it is assumed that all connections between the material points are preserved, there is no damage in the structure. If $\beta = 0$, a local rupture is considered, since all connections between the material points were removed.

In the present model, it is considered that the damage affects only the elastic properties of the structure, so that the stiffness matrix obtained by the finite element method is given by Eq. (11)

$$\mathbf{K}(\beta_{\mathbf{h}}) = \int_0^{l_x}\int_0^{l_y} \beta_h(x,y)B^T(x,y)\,E_0\,B(x,y)\,dx\,dy, \tag{11}$$

where,

$$E_0 = \frac{E}{1-\nu^2}\begin{bmatrix} 1 & \nu & 0 \\ \nu & 1 & 0 \\ 0 & 0 & \mu \end{bmatrix}, \tag{12}$$

$$\mu = \frac{1-\nu}{2} \tag{13}$$

and

$$B = \begin{bmatrix} \frac{\partial^2}{\partial x^2} \\ \frac{\partial^2}{\partial y^2} \\ 2\frac{\partial^2}{\partial x \partial y} \end{bmatrix} N. \tag{14}$$

In these equations, l_x and l_y corresponds to the lengths of the plate in the axes x and y, respectively, β_h is the approximation of the field β obtained from its spatial discretization, B is the differential discrete operator, N a matrix containing the interpolation functions, E and ν are, respectively, the elastic modulus and Poisson's ratio.

In this paper, the discretization of the field β used the same mesh of the displacement field. It should be noted that the discretization of the field $\beta(x, y)$ does not depend on the discretization of the displacement field, so that different meshes can be adopted.

It was considered that the field $\beta(x, y)$ for each finite element of the plate is interpolated by four nodal values, see Fig. 1.

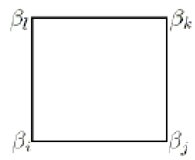

Figure 1. Distribution of the nodal cohesion paramters in the rectangular element.

The problem of damage identification can be defined as an optimization problem where the following functional must be minimized

$$\min_{\beta} \ \mathcal{F}, \ \text{satisfying} \ 0 \leq \beta \leq 1 \tag{15}$$

with,

$$\mathcal{F}(\beta) = \frac{\|\bar{\mathbf{G}}_{\text{exp}} - \bar{\mathbf{G}}\|^2}{2\|\bar{\mathbf{G}}_{\text{exp}} - \bar{\mathbf{G}}_0\|}, \tag{16}$$

where $\bar{\mathbf{G}}_0$ is the reduced flexibility matrix computed with the inicial estimate of the field β.

In order to present a more direct interpretation of the damage described by the cohesion parameter β, the damage parameter D is defined, which represents the intensity of the damage as

$$D = 1 - \beta. \tag{17}$$

3. OPTIMIZATION METHOD

In the damage identification problem proposed, the aim is the minimization over the cohesion parameter β of an error based on the difference between the experimental flexibility matrix and the original flexibility matrix of the FEM. For this, it will be used the optimization method described in this Section.

3.1 Luus-Jaakola Method

The basic idea of the stochastic algorithm of Luus & Jaakola (1973), is to select random solutions in a region that decreases in size over the course of iterations, as the pseudocode below.

Choose the size of initial search r^0;
Choose the number of internal n_{int} and external loops, n_{ext};
Choose the contraction coefficient c;
Choose the initial solution $\beta^* = \beta_0$

For $i = 1 : n_{\text{ext}}$
For $j = 1 : n_{\text{int}}$
$\beta^j = \beta^* + R^j r^{(j-1)}$, where R is a diagonal matrix consisted by random numbers between -0,5 and 0,5
If $\mathcal{F}(\beta^j) < \mathcal{F}(\beta^*)$
$\beta^* = \beta^j$
end (If)
end (For)
$r^i = (1 - c) r^{(i-1)}$
end (For)

4. RESULTS

In this paper, it was considered a clamped aluminum plate $0,5\,\text{m}$ long, $0,005\,\text{m}$ thick, $0,5\,\text{m}$ wide, nominal elastic modulus $E_0 = 7.2582 \times 10^{10}$ Pa and Poisson's ratio $\nu = 0.33$.

The plate was discretized by the finite element method in 64 elements, where each element has four nodes and each nodal point has three degrees of freedom: one transverse (v), one rotation in x (θ_x) and one rotation in y (θ_y). The structure has a total of 81 nodes and 216 DOF, because nine nodes of the structure stay in the clamped side.

The imposition of the damage to the beam is accomplished through the β parameter that describes the damage. In the damaged nodes we have $\beta \neq 1$ (ou $D \neq 0$), and the in the nodes where there are no damages $\beta = 1$ (ou D = 0). The FEM with the required values of the cohesion parameter is used to generate the frequencies and vibration modes of the damaged structure, thus representing the experimental data.

Three different damage scenarios were considered: only one damaged region, two adjacent damaged regions and two distant damaged regions. Table 1 shows the cases considered.

Table 1. Damage Scenarios

CASE	POSITION	DAMAGE (D)
1	12	0.4
2	19	0.2
3	33	0.2
4	35	0.3
5	41	1
6	76	0.2
7	30; 39	0.2; 0.3
8	21; 47	0.2; 0.2
9	12; 66	0.2; 0.4

Since the Luus-Jaakola method consists of a random search, it showed a considerable sluggish to update at once all the 81 parameters of the model. For this reason, it was used a technique to locate the damaged region before the use the optimization method and thus diminished the quantity of parameters to be updated and therefore the runtime of the model.

Because the flexibility matrix is the inverse of the stiffness matrix, the product of the experimental flexibility matrix by the reduced stiffness matrix for a structure without damage, will result in an identity matrix. Therefore, for the location of the damage structure, we have

$$\mathbf{L} = \bar{\mathbf{G}}_{\text{exp}} \bar{\mathbf{K}} - \mathbf{I}, \tag{18}$$

so when all of the DOF of the structure are measured in the modal test, if the structure has any damaged component, only the DOF of these elements will have values different from zero.

A vector of localization $\mathbf{P}_{\text{j}}$ can be defined, so that its *j-th* component corresponds to the sum of the modules of the components that form the *j-th* column of matrix $\mathbf{L}$, then

$$\mathbf{P}_{\text{j}} = \sum_{i=1}^{m} |\mathbf{L}_{\text{i,j}}|, \tag{19}$$

where m is the total number of measured DOF.

Since not all DOF and vibration modes were considered as measured in the modal test, what we get by Eq. (19) is the profile of the DOF to the structure without damage, thus to be subtracted from the result of Eq. (19) to the structure with damage, there is an abrupt change from the DOF related to the damage. Thus it was possible to reliably identify the damaged region.

In this paper, only the transverse DOF were considered as measured and the first 10 vibration modes were taken. In Fig. 2 it is presented, in black and red, respectively, the distribution of the cohesion parameters and the transverse DOF of the structure.

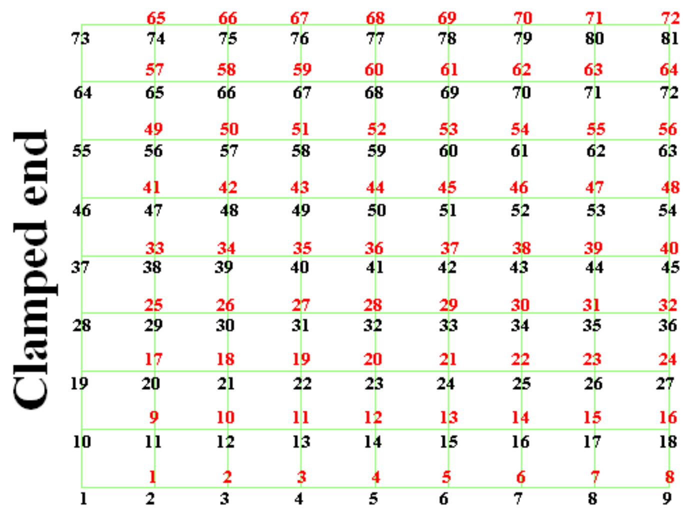

Figure 2. Distribution of transversal DOF and cohesion parameters.

In Fig. 3 the first simulation result is shown. The damage was imposed at node 12, case 1, with D = 0.4. In Fig. 2a it is depicted the vector of localization, $\mathbf{P}_\mathrm{j}$, showing an abrupt change around the tenth DOF. Looking to Fig. 3, it can be see that the nine nodes around node 12 (nodes 2, 3, 4, 11, 12, 13, 20, 21 and 22) should be upgraded. In Fig. 3b it is shown the result of the Luus-Jaakola optimization method updating only the region indicated earlier. As can be seen, the location and severity of the damage are indicated precisely.

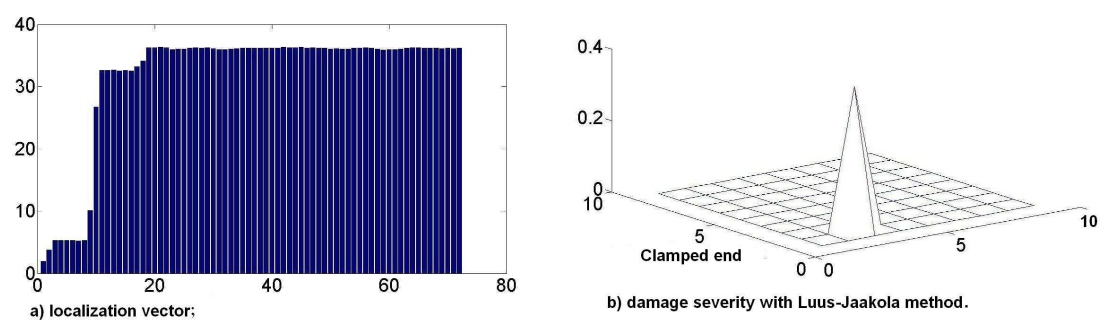

Figure 3. Damage identification for Case 1.

In Fig. 4, the result of the simulation of damage at the clamped line is shown. The damage was imposed at the node 19, through the damage value (D) 0.2. A sudden change is observed next to the DOF 17 and that corresponds to the region of the cohesion parameter 20 (see Fig. 2). The parameters of this region were updated and identified precisely the damage.

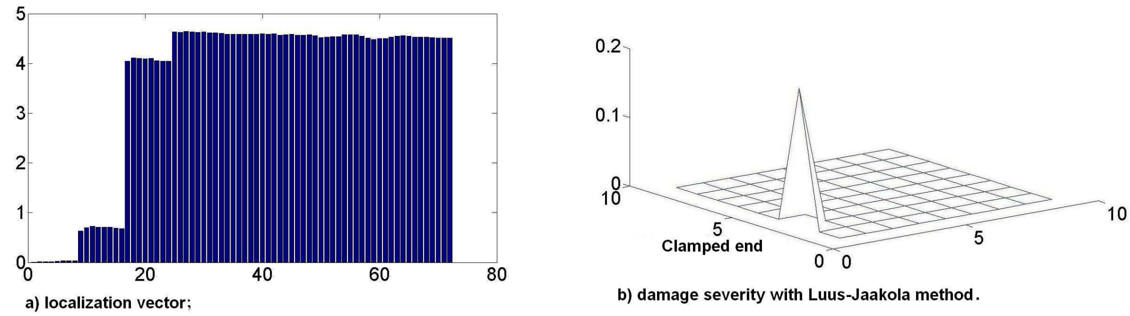

Figure 4. Damage identification for Case 2.

In Fig. 5a, the result of simulation where the damage was imposed at the node 33 through the damage value (D) 0.2 is shown. In this case the DOF 29 was the first to introduce a sudden change and is associated to the node 33 where the damage is located. The parameters 23, 24, 25, 32, 33, 34, 41, 42 and 43 were updated as they were in the indicated region and identified the damage properly, as shown in Fig. 5b.

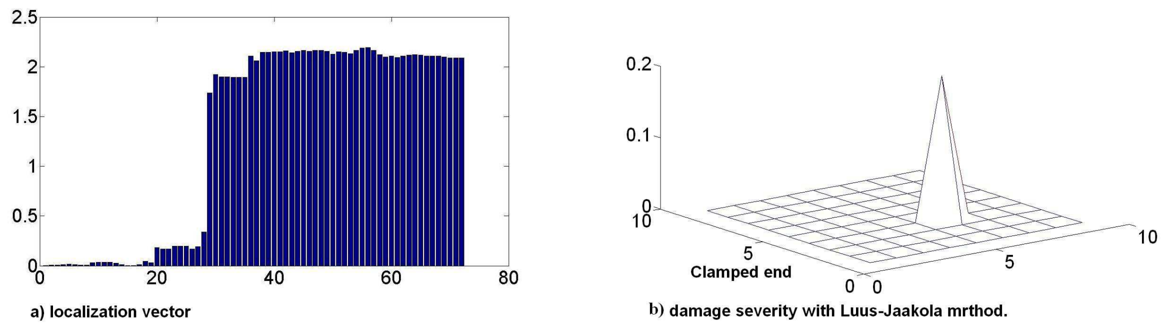

Figure 5. Damage identification for Case 3.

In Fig. 6, the result of the simulation of a damage in a free end of the plate and parallel to the clamp is presented. The damage was imposed at node 35 through the damage value (D) 0.3. It is observed an abrupt change in the DOF 31, which corresponds to location of damage and, when using the Luus-Jaakola method to update the parameters of this region, the damage was correctly identified. In this case, the updated parameters were at nodes 25, 26, 27, 34, 35, 36, 43, 44 and 45.

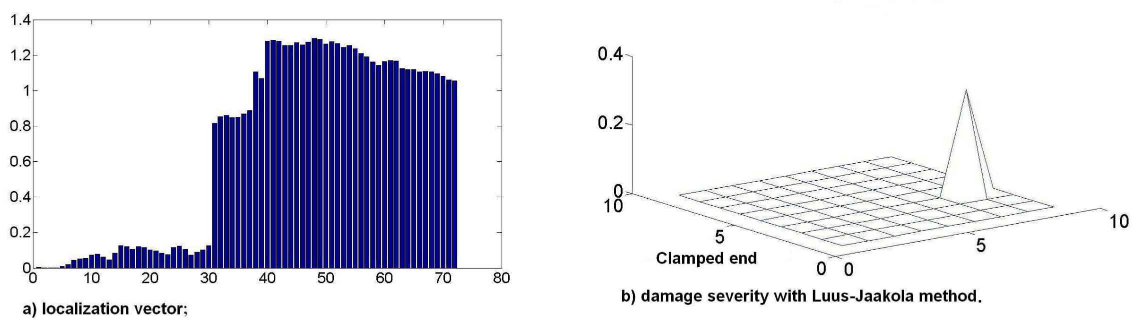

Figure 6. Damage identification for Case 4.

In Fig. 7, it was simulated the appearance of a hole in the center of the plate, where the damage was imposed at the node 41, through the damage value D = 1. An abrupt change in $\mathbf{P}_j$ is observed next to the DOF 36, the parameters 31, 32, 33, 40, 41, 42, 49, 50 and 51 were updated. In Fig. 7b it is shows that the damage has been identified with precision.

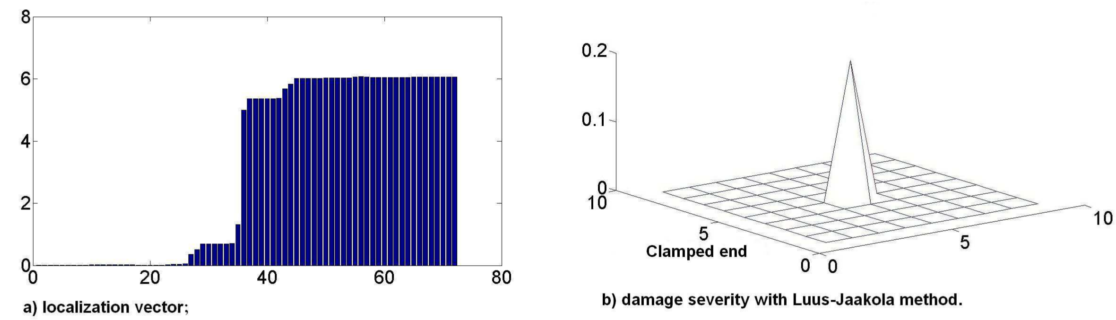

Figure 7. Damage identification for Case 5.

Another area where it was simulated the presence of a damage is shown in Fig. 8. In this case the damage was imposed at the node 76, through the damage value (D) 0.2. Again the region indicated is really the damaged area. We updated the parameters 66, 67, 68, 75, 76 and 77 and the damage was identified accurately.

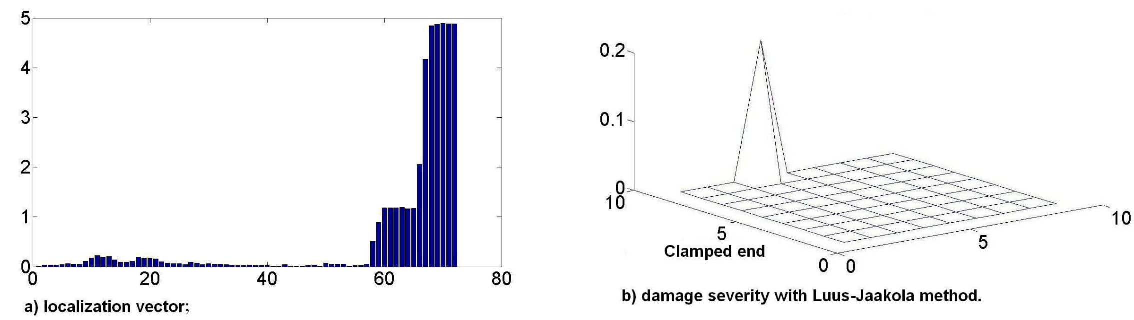

Figure 8. Damage identification for Case 6.

In Fig. 9, the result of a simulation where the damage was imposed on nodes 30 and 39 through the values of damage (D) 0.4 and 0.1, respectively, is depicted. We have then, a case where two adjacent regions are damaged. Notice that on Fig. 9a, two regions suddenly change their values next to the DOF 26 and 34. The parameters 29, 30, 31, 38, 39, 40, 47, 48 and 49 were updated. Once more, the damage was correctly identified, as it can be seen in Fig. 9b.

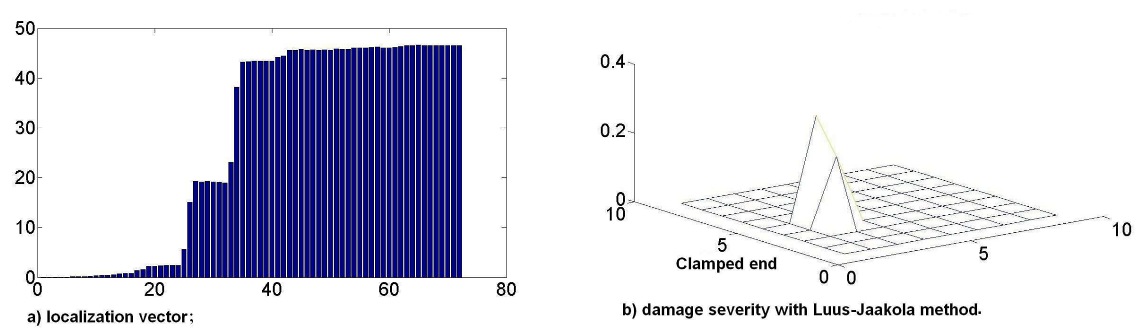

Figure 9. Damage identification for Case 7.

In the cases presented in Figs. 10 and 11, one has the case of two damaged regions again but now the nodes where the damages were imposed are far apart. You can check that on the left of both figures, there are two regions that show considerable variation. For the case shown in Fig. 10, the damage was imposed on the nodes 21 and 47, through the values of damage (D) 0.2 in both. The parameters 20, 21, 22, 46, 47 48 were updated. For the case shown in Fig. 11, the damage was imposed on the nodes 12 and 66, through the values of damage (D) 0.2 and 0.4 respectively. In this case, the parameters: 11, 12, 13, 65, 66 and 67 were updated. In either case, we found results that accurately identify the location and severity of the damage.

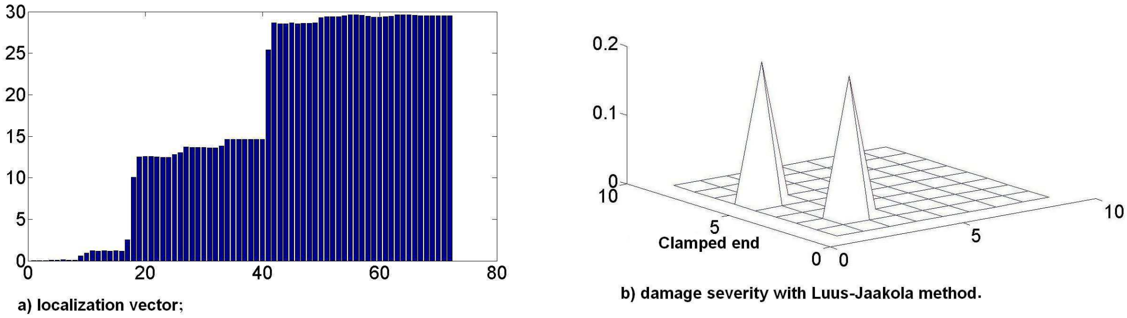

Figure 10. Damage identification for Case 8.

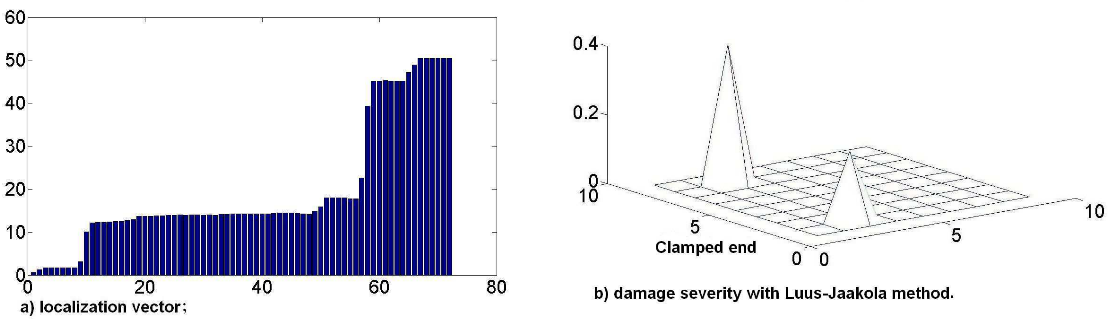

Figure 11. Damage identification for Case 9.

5. CONCLUSIONS

The method of identifying damage via flexibility matrix performed satisfactorily in the case of rectangular plates, being able to accurately identify the location and severity of the damage. The Luus-Jaakola method, as it is a method that randomly chooses the solution of the proposed problem, demonstrated considerable slowness in finding the solution when a large number of parameters are updated. For this reason, the flexibility matrix itself was used to provide an estimation of the damage localization, and thus allowing a smaller number of parameters to be updated by the model, allowing to locate and quantify the damage properly. It is important to highlight that all the transverse DOF were considerated as "measured" in this work and, for this reason, it was a simple task to associate the DOF that changed abruptly with the damaged parameter. However, in practice, we seek to work with a small number of sensors, not allowing to obtain information from all the DOF. This problem will be addressed in a future work.

6. REFERENCES

Alvandi, A., & Cremona, C., 2006. Assessment of vibration-based damage identification techniques. *Journal of Sound and Vibration*, 202, pp. 179–202.

Alvin, K. F., Peterson, L. D, & Park, K. D., 1995. Method for determining minimum-order mass and stiffness matrices from modal test data. *AIAA Journal*, vol. 1, n. 33, pp. 128–135.

Carrilo, O. J. B. & Laier, J. E., 2006. Detecção de dano a partir da resposta dinâmica da estrutura: estudo analítico com aplicação a estrutura do tipo viga. *Cadernos de Engenharia de Estruturas*, São Carlos, ISSN 1809-5860, vol. 8, n. 35, pp. 29–45.

Chang, P. C., Flatau, A., & Liu, S. C., 2003. Review Paper: Health monitoring of civil infrastructure. In *structural health monitoring*, vol. 2 n. 3, pp. 257–267.

Guyan, R. J., 1965. Reduction of stiffness and mass matrices. *AIAA Journal*, vol. 3 n. 2, pp. 380.

Jauregui, D. V. & Farrar, C. R., 1996. Comparison of damage identification algorithms on experimental modal data from a bridge. *14th International Modal Analysis Conference Dearborn*. Michigan February 12-15.

Luus, R. & Jaakola, T., 1996. Optimization by direct search and systematic reduction of the size of search region. *AIChE Journal*, vol. 19, pp. 760–766.

Stutz, L. T., Castello, D. A., Rochinha, F. A. 2005. A flexibility-based continuum damage identification approach. Journal of Sound and Vibration, 279, pp. 641-667

7. ACKNOWLEDGEMENTS

The authors thank to the Labortório de Instrumentação em Dinâmica, Acústica e Vibrações (LIDAV), of the Instituto Politécnico of the Universidade do Estado do Rio de Janeiro (UERJ), to the Universidade Federal Fluminense (UFF), and the Fundação Carlos Chagas Filho de Amparo à Pesquisa do Estado do Rio de Janeiro (FAPERJ).

8. Responsibility notice